

## Comparative Phototransformation of Environmental Pollutants Using Metallophthalocyanines Supported on Electrospun Polymer Fibers

Ruphino Zugle, Tebello Nyokong

Department of Chemistry, Rhodes University, Grahamstown 6140, South Africa

Correspondence to: T. Nyokong (E-mail: t.nyokong@ru.ac.za)

**ABSTRACT:** The fluorescence and photoactivity of a series of Zn and Lu phthalocyanine complexes incorporated in various polymer fibers were investigated for the phototransformation of 4-chlorophenol, 4-nitrophenol, and methyl orange. The phthalocyanine complexes functionalized on polystyrene and polysulfone polymer fibers could be applied in the degradation of 4-chlorophenol, 4-nitrophenol, and methyl orange with 4-chlorophenol being much more susceptible to degradation while methyl orange was the least. Also polymer fibers of polystyrene were found to be reusable. © 2012 Wiley Periodicals, Inc. *J. Appl. Polym. Sci.* 128: 1131–1142, 2013

**KEYWORDS:** zinc phthalocyanine; electrospinning; methyl orange; chlorophenol; nitrophenol; photocatalysis

Received 27 April 2012; accepted 21 July 2012; published online 9 August 2012

DOI: 10.1002/app.38381

### INTRODUCTION

Detection of analytes including those of environmental concern is often done using functional molecules that are either chemically linked or adsorbed on appropriate substrate to promote selectivity and sensitivity.<sup>1–3</sup>

Phthalocyanines (Pcs) possess electrochemical and photophysical properties that make them very interesting functional molecules for sensing analytes such as environmental pollutants. Currently, emphasis is being placed on advanced oxidation processes<sup>4</sup> for environmental remediation and in particular for water treatment. Photochemical oxidation using molecular oxygen is one of the most important methodologies, since it does not liberate any additional pollutants. Singlet oxygen is a particularly good candidate for these applications. It is a very reactive species, as can be seen from its applications in areas such as photodynamic therapy.<sup>5</sup> Phthalocyanines have been shown to be highly effective photosensitizers capable of producing singlet oxygen with high quantum yields.<sup>6</sup> Pcs are particularly very promising sensitizers since their maximum light absorption occurs in the visible region which constitutes a larger portion of the spectrum.<sup>7,8</sup>

The use of phthalocyanine (Pc)-containing polymer fibers in solving environmental problems is an ongoing exciting challenge. The physical and chemical properties of the polymers could be very useful in enhancing the desired properties of the resulting functionalized fibers. For instance poly(ethylene oxide) (PEO) is an effective ion conductive polymer, hence it could facilitate preparation of optoelectronic fibrous materials.<sup>9,10</sup> Also

materials consisting of polyacrylonitrile nanofibers are reported to show super hydrophobicity and/or catalytic properties.<sup>11,12</sup> Thus, the choice of the polymer type and the morphology of the corresponding functionalized fibers should be closely related to the desired application.

ZnPc and CuPc complexes have been previously incorporated into polyurethane and poly(ethylene oxide) polymers, respectively,<sup>13,14</sup> but applications towards photocatalysis were not explored especially for the ZnPc derivative, which is photoactive. We have recently examined LuPc and ZnPc derivatives (when used to functionalize polyacrylic acid or polystyrene) toward the detection of nitrogen dioxide and for phototransformation of 4-chlorophenol and 4-nitrophenol.<sup>15–17</sup> In this work, therefore, we present a comparative analysis of the suitability of various polymers: polystyrene (PS), polyacrylic acid (PAA), polysulfone (PSU), and polyurethane (PUR) functionalized with Zn and Lu phthalocyanine complexes for the phototransformation of 4-chlorophenol, 4-nitrophenol and methyl orange, all are known pollutants. In particular, the reusability of the functionalized fibers as well as the relative ease of phototransformation of the pollutants will be investigated.

### EXPERIMENTAL

#### Materials

The following chemicals were purchased from SAARCHEM: 1-pentanol, *n*-hexane, and *N,N*-dimethylformamide (DMF). Zinc phthalocyanine (ZnPc), benzoquinone, 4-nitrocatechol, 4-nitrophenol (4-NP), polystyrene (PS) polysulfone (PSU), methyl orange (MO), polyacrylic acid (PAA) ( $M_w = 450,000 \text{ g mol}^{-1}$ ),

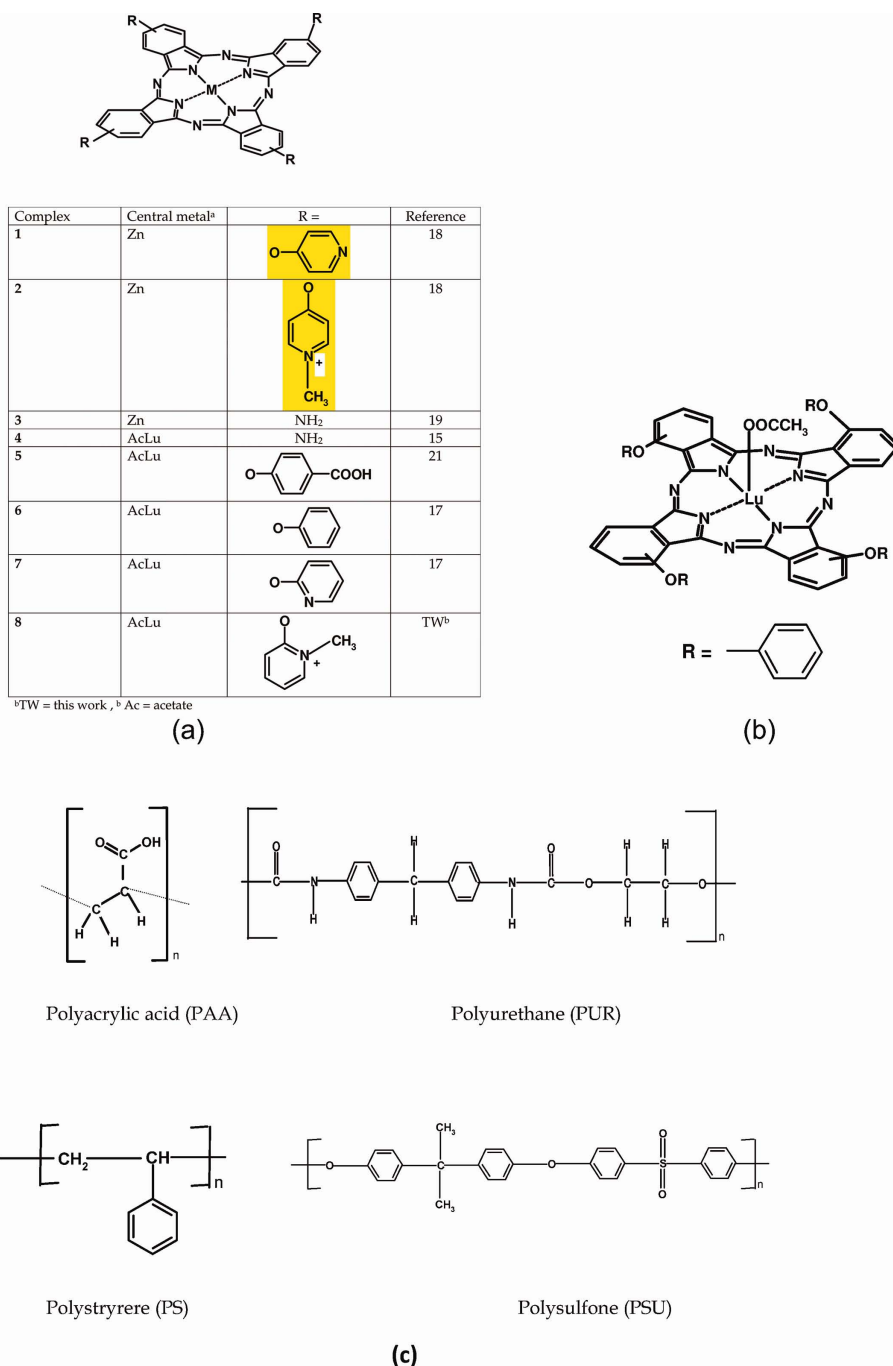
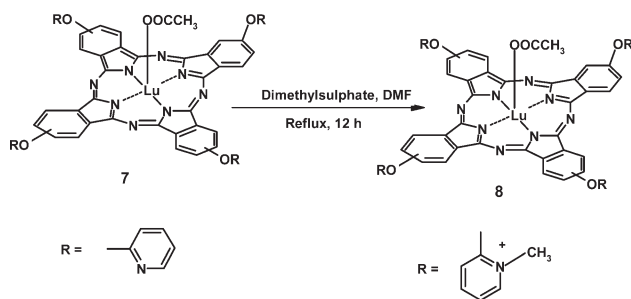


**Figure 1.** (a) Structure of peripherally substituted Pcs used in this work. (b) The structure of nonperipherally substituted complex **9**. (c) Unit structures of all polymers used in this work. [Color figure can be viewed in the online issue, which is available at [wileyonlinelibrary.com](http://wileyonlinelibrary.com).]

polyurethane (PUR) (average molecular weight 5000, specific gravity 1.14), metallic copper, dimethyl sulfate, 3-diphenylisobenzofuran (DPBF), anthracene-9,10-bis-methylmalonate (ADMA), and 1,8-diazabicyclo[5.4.0] undec-7-ene (DBU), were from Sigma–Aldrich. The 4-chlorophenol (4-CP), (99%) was from Fluka. Hydroquinone was from May and Baker. Ultrapure water (Milli-Q water system, Millipore, Bedford, MA) was used for all photocatalyzed aqueous solutions. Phosphate buffer solutions were prepared using reagent grade potassium dihydrogen

orthophosphate (ACE) and dipotassium phosphate (PAL chemicals). Figure 1 shows all the phthalocyanine and polymer structures. The phthalocyanines are: zinc(II) 2(3), 9(10), 16(17), 23(24)-(tetrapyriddyloxy)]-phthalocyanine (**1**),<sup>18</sup> zinc(II) 2(3), 9(10), 16(17), 23(24)-tetrakis[4-(*N*-methylpyridyloxy)]-phthalocyanine (**2**),<sup>18,19</sup> zinc 2(3), 9(10), 16(17), 23(24)-tetraaminophthalocyanine (**3**),<sup>20</sup> 2(3), 9(10), 16(17), 23(24)-(tetraaminophthalocyaninato) lutetium acetate (**4**),<sup>15</sup> 2(3), 9(10), 16(17), 23(24)-(tetracarboxyphenoxyphthalocyaninato) lutetium acetate



Scheme 1. Synthetic route for complex 8.

(5)<sup>21</sup> 2(3), 9(10), 16(17), 23(24)-(phenoxyphthalocyaninato) lutetium acetate (6), 2(3), 9(10), 16(17), 23(24)-(tetrapyriddyloxphthalocyanato lutetium acetate (7)<sup>17</sup> and 1(4), 8(11), 15(18), 22(25)-(tetraphenoxyphthalocyaninato) lutetium acetate (9),<sup>22</sup> and were synthesized according to literature procedures. Synthesis of 2(3), 9(10), 16(17), 23(24)-tetrakis[4-(*N*-methylpyridiloxy) phthalocyaninato] lutetium acetate (8) is described in this work, Scheme 1.

### General Equipment

Infrared (IR) spectra were recorded on a Perkin–Elmer Fourier transform–IR (100 FT-IR) spectrophotometer. UV–vis absorption spectra were recorded on a Shimadzu UV-2550 spectrophotometer. Fluorescence excitation and emission spectra were recorded on a Varian Cary Eclipse spectrofluorimeter. <sup>1</sup>H NMR spectra were recorded on a Bruker AMX600 MHz in D<sub>2</sub>O. Microanalyses were performed using a Vario-Elementar Microcube ELIII. Mass spectral data were recorded on ABI Vogager De-STR Maldi TOF instrument using  $\alpha$ -cyano-4-hydroxycinnamic acid as a matrix.

Irradiations for singlet oxygen studies were done using General Electric Quartz lamp (300 W), 600-nm glass (Schott) and water filters, to filter off ultraviolet and far infrared radiations, respectively. An interference filter 670 nm with bandwidth of 40 nm was placed in the light path just before the cell containing the sample.

Fluorescence images of the fibers were taken with a DMLS fluorescence microscope. The excitation source was a high-voltage mercury lamp and light in the wavelength range of 550–730 nm was employed. Scanning electron microscope (SEM) images were obtained using a JOEL JSM 840 scanning electron microscope.

### Photophysical and Photochemical Parameters

**Fluorescence Quantum Yield.** Fluorescence quantum yield ( $\Phi_F$ ) of the phthalocyanine (8) was determined in DMF by the comparative method,<sup>23</sup> eq. (1)

$$\Phi_F = \Phi_F^{\text{Std}} \frac{FA_{\text{Std}}I^2}{F_{\text{Std}}A_{\text{Std}}I^2} \quad (1)$$

where  $F$  and  $F_{\text{Std}}$  are the areas under the fluorescence emission curves of sample (8) and the standard, respectively.  $A$  and  $A_{\text{Std}}$  are the respective absorbances of the sample and standard at the excitation wavelength. The same solvent was used for sample and standard. Unsubstituted ZnPc in DMF ( $\Phi_F^{\text{Std}} = 0.30$ )<sup>24</sup> was

employed as the standard. Both the sample and standard were excited at the same wavelength of 612 nm and emission spectrum was recorded from 620 to 790 nm. The absorbances of the solutions at the excitation wavelength were about 0.05 to avoid any inner filter effects.

**Singlet Oxygen Quantum Yield.** A chemical method was employed to determine the singlet oxygen quantum yield,  $\Phi_{\Delta}$ , of complex 8 in DMF. The comparative method was used with ZnPc ( $\Phi_{\Delta}^{\text{ZnPc}} = 0.56$  in DMF),<sup>25,26</sup> as standard and DPBF as singlet oxygen quencher, using eq. (2):

$$\Phi_{\Delta} = \Phi_{\Delta}^{\text{ZnPc}} \cdot \frac{R^{\text{Sample}}}{R^{\text{ZnPc}}} \cdot \frac{I^{\text{ZnPc}}}{I^{\text{Sample}}} \quad (2)$$

where  $\Phi_{\Delta}^{\text{ZnPc}}$  is the singlet oxygen quantum yield for the ZnPc standard,  $R^{\text{Sample}}$  and  $R^{\text{ZnPc}}$  are the DPBF photobleaching rates in the presence of complex 8 and ZnPc standard, respectively, while  $I^{\text{Sample}}$  and  $I^{\text{ZnPc}}$  are the respective rates of light absorption by complex 8 and the ZnPc standard. The initial DPBF concentrations were kept the same for both the standard and the sample. Molar extinction coefficient of DPBF at  $\lambda = 417$  nm in DMF  $\epsilon = 23,000$  (dm<sup>3</sup> mol<sup>-1</sup> cm<sup>-1</sup>).<sup>27</sup>

For the modified fibers (reported for the first time in this work); PSU/ZnPc, PSU/complex 1, PSU/complex 2 and PS/complex 8, the singlet oxygen quantum yields ( $\Phi_{\Delta}$ ) determination were carried out in aqueous solutions using ADMA as the quencher and its degradation was monitored at 380 nm. An amount of 10 mg of the modified fiber in each case was suspended (as small pieces) in an aqueous solution of ADMA and irradiated using the photolysis set-up described above. The quantum yield ( $\Phi_{\text{ADMA}}$ ) was estimated using eq. (3), using the extinction coefficient of ADMA in water  $\log(\epsilon) = 4.1$ .<sup>28</sup>

$$\Phi_{\text{ADMA}} = \frac{(C_0 - C_t)V_R}{I_{\text{abs}} \cdot t} \quad (3)$$

where  $C_0$  and  $C_t$  are the ADMA concentrations prior to and after irradiation, respectively;  $V_R$  is the solution volume;  $t$  is the irradiation time per cycle and  $I_{\text{abs}}$  is defined by eq. (4):

$$I_{\text{abs}} = \frac{\alpha \cdot A \cdot I}{N_A} \quad (4)$$

where  $\alpha = 1 - 10^{-A(\lambda)}$ ,  $A(\lambda)$  is the absorbance of the sensitizer at the irradiation wavelength,  $A$  is the irradiated area (2.5 cm<sup>2</sup>),  $I$  is the intensity of light ( $4.54 \times 10^{16}$  photons cm<sup>-2</sup> s<sup>-1</sup>) and  $N_A$  is Avogadro's constant.

The absorbance used for eq. (4) is that of the phthalocyanine in the fiber (not in solution) measured by placing the modified fiber directly on a glass plate. The light intensity measured refers to the light reaching the spectrophotometer cell, and it is expected that some of the light may be scattered, hence the  $\Phi_{\Delta}$  values of the phthalocyanine in the fibers are estimates. The singlet oxygen quantum yields ( $\Phi_{\Delta}$ ) were calculated using eq. (5)<sup>29</sup>

$$\frac{1}{\Phi_{\text{ADMA}}} = \frac{1}{\Phi_{\Delta}} + \frac{1}{\Phi_{\Delta}} \cdot \frac{k_d}{k_a} \cdot \frac{1}{[\text{ADMA}]} \quad (5)$$

where  $k_d$  is the decay constant of singlet oxygen in respective solvent and  $k_a$  is the rate constant of the reaction of ADMA with  $O_2(^1\Delta_g)$ . The intercept obtained from the plot of  $1/\Phi_{ADMA}$  versus  $1/[ADMA]$  gives  $1/\Phi_{\Delta}$ .

### Photocatalytic Reactions

Photocatalytic reactions were carried out in a magnetically stirred batch reactor (glass vial). The irradiation experiments were carried out using the photolysis set-up described above for singlet oxygen detection. The intensity of the light reaching the reaction vessel was measured with a power meter (POWER MAX 5100, Molelectron Detector) and found to be  $3.52 \times 10^{20}$  photons  $cm^{-2} s^{-1}$ . The transformations were monitored by observing the absorption bands at 243 and 297 nm for 4-CP, 400 nm for 4-NP and 470 nm for methyl orange after each photolysis cycle of thirty minutes using a Shimadzu UV-2550 spectrophotometer. The experiments were carried out using a variety of concentrations of 4-chlorophenol in pH 11, 4-nitrophenol in pH 8.2, and methyl orange in pH 9.2 aqueous buffer solutions. Each sample solution (4 mL) contained 20 mg of functionalized fiber, suspended in small pieces.

### Chromatographic Analysis

The photolysis products were analyzed using gas chromatography (GC) and/or by direct injection into ion trap mass spectrometer fitted with an electrospray ionization (ESI-MS) mass source. For gas chromatographic analysis, an Agilent Technologies 6820 GC system fitted with a DB-MS Agilent J & W GC column was employed. A Finnigan MAT LCQ ion trap mass spectrometer equipped with an electrospray ionization (ESI) source was used for mass analysis. Spectra were acquired in the negative ion mode, with the capillary temperature set at 200°C and sheath gas set at 60 arbitrary units, with the capillary and tube lens voltage set at -20 and -5 V, respectively. The photocatalyzed aqueous sample solution was extracted with dichloromethane in the case of 4-chlorophenol and 4-nitrophenol and then injected into the GC. However sample solutions of methyl orange were directly injected into the ion trap mass spectrometer.

### Synthesis

Synthesis of 2,(3), 9(10), 16(17), 23(24)-tetrakis[4-(*N*-methylpyridiloxy)-phthalocyaninato] lutetium acetate (8), Scheme 1.

This complex was synthesized following a reported procedure for forming quarternized phthalocyanines.<sup>30</sup> Complex (7)<sup>17</sup> (100 mg, 0.09 mmol) was dissolved in freshly distilled DMF and the solution was heated under reflux. Dimethylsulfate (0.2 mL) was added drop-wise. The resulting mixture was then heated under reflux for 12 h after which the solution was cooled and the product precipitated with chloroform. The resulting solid product was purified by Soxhlet extraction with acetone.

Yield: 21%, IR ( $cm^{-1}$ ): 761, 857, 953, 1001, (Pc skeleton), 1042 S=O), 1246, 1341, 1355 (C—O—C), 1482, 1472, (S=O), 1633, 1777 (acetate), 2795, 2957 (C—H aromatic), 3063 (CH<sub>3</sub>), 3428 (H<sub>2</sub>O); <sup>1</sup>H NMR (D<sub>2</sub>O):  $\delta$ , ppm 8.91–9.44 (28 H, m, Pc-H, and Pyridyl-H), 4.11–4.33 (12 H, m, Pyridyl-CH<sub>3</sub>), 2.09 (3 H, s, acetate-CH<sub>3</sub>); Calcd for C<sub>58</sub>H<sub>43</sub>N<sub>12</sub>O<sub>22</sub>S<sub>4</sub>Lu 2(H<sub>2</sub>O); C 43.56%, H 2.84%, N 10.51%, S 8.02%, Found C 43.63%, H 2.93%, N

10.35% S 8.51%; UV-Vis (DMF):  $\lambda_{max}$  nm (log  $\epsilon$ ) 353 (4.55), 614 (4.41), 680 (5.68); (ES<sup>+</sup>), (*m/z*); Calcd 1563; Found 1548 [M-CH<sub>3</sub>]<sup>+</sup>.

### Preparation of Functionalized Fibers

**Polystyrene (PS) Polymer Fibers.** The fibers were prepared as reported before<sup>16</sup> by mixing the phthalocyanine with the polymer solution and the mixture electrospun into fibers. The same concentration of the particular Pc was added in each polymer solution for easy comparison. Briefly, the following conditions were used: a solution containing 2.5 g ( $1.3 \times 10^{-5}$  moles) of polystyrene (PS) and the mass equivalent of  $1.2 \times 10^{-6}$  moles of the functional phthalocyanine in 10 mL DMF/THF(4 : 1) was stirred for 24 h to produce a homogeneous solution. The phthalocyanines which were employed (as examples) for studies with this polymer are complexes (6, 7, 8, 9) and ZnPc. These will show the effect of the nature of the substituent and the point of substitution. ZnPc was employed as a common Pc for comparison. Each solution was then placed in a cylindrical glass tube fitted with a capillary needle. A potential difference of 20 kV was applied to provide charge for the spinning process. The distance between the cathode (static fiber collection point) and anode (tip of capillary needle) was 15 cm and pump rate of 0.02 mLh<sup>-1</sup>.

**Polysulfone (PSU) Polymer Fibers.** As was the case with PS above, the fibers were prepared by mixing the phthalocyanine with the polymer solution and then electrospun as reported before<sup>31</sup> with modifications as follows: a solution containing 2.0 g of polysulfone (PSU) and 1.35 mg of the complex 1, 2, 7 or ZnPc in 10 mL DMF/THF(4 : 1) was stirred for 24 h to produce a homogeneous solution. These phthalocyanines were employed (as examples) for this polymer. This polymer allows for the interaction between the aromatic systems of the Pc and the polymer, hence preventing leaching of the former from the latter during application. The solution was then placed in a cylindrical glass tube fitted with a capillary needle. A potential difference of 20 kV was applied to provide charge for the spinning process. The distance between the cathode (static fiber collection point) and anode (tip of capillary needle) was 10 cm and pump rate was 0.5 mLh<sup>-1</sup>. Similar conditions were applied to obtain fiber of the polysulfone alone.

**The Linking of Pc Complexes to Polyurethane (PUR) Polymer and Polyacrylic Acid (PAA).** Complex 5 was employed since it contains carboxyl substituents which allow for the chemical linking with the amino group of the PUR polymer, while complexes 3 and 4 containing amino substituents were employed for the PAA polymer. Experiments were also performed where complexes 3, 4, and 5 or ZnPc were mixed with the respective polymers without the formation of a chemical bond. For the chemical linking of phthalocyanine to PUR and PAA we followed the procedure we reported before.<sup>15,21</sup> Electrospinning conditions were also as reported before.<sup>15,21</sup>

## RESULTS AND DISCUSSION

### Characterization of Complex 8

The phthalocyanine complex was synthesized and characterized according to the procedure described in literature.<sup>30</sup> A

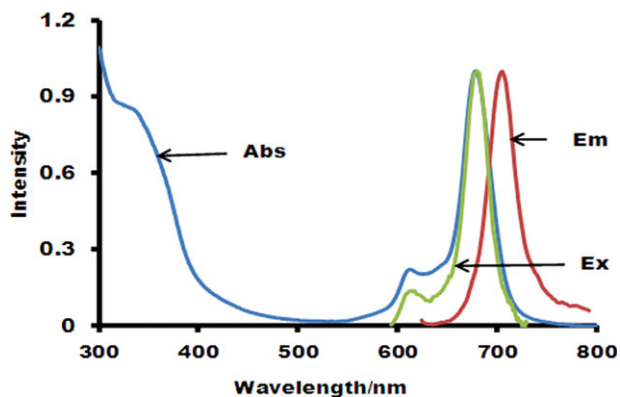


**Figure 2.** absorption (abs), emission (em), and excitation (Ex) spectra for complex **8** in DMF. [Color figure can be viewed in the online issue, which is available at [wileyonlinelibrary.com](http://wileyonlinelibrary.com).]

molecular ion 1548 amu corresponding to  $[M+CH_3]^+$  was obtained. The complex is quite soluble in water confirming its ionic nature. The presence of the sulfate counter anion was confirmed with the barium chloride test. Infrared and  $^1H$  NMR as well as elemental analysis jointly confirmed the structure.

The UV–visible spectrum in DMF, Figure 2, shows a monomeric behavior with a narrow Q band, with Beer–Lambert law obeyed below  $1 \times 10^{-5}$  M. Q-band maximum was observed at 680 nm. Figure 2 shows that the excitation spectrum is similar to the absorption spectrum and both are a mirror image of emission spectrum of the complex. Also it can be observed that the absorption and excitation spectral bands are in close proximity suggesting that the nuclear configuration of the ground and excited states of the complex are not affected by excitation.

The fluorescence quantum yield ( $\Phi_F$ ) was determined using unsubstituted zinc phthalocyanine as standard and a value of  $\Phi_F < 0.01$  was obtained. Similar low fluorescence quantum yields of Lu phthalocyanine complexes have been reported<sup>21,22</sup> and attributed to the heavy atom effect. A similar reason has also been assigned to phthalocyanine complexes of hafnium which do not fluoresce at all.<sup>32</sup>

The singlet oxygen quantum yields were determined both in solution (DMF) and in a solid polystyrene polymer fiber matrix

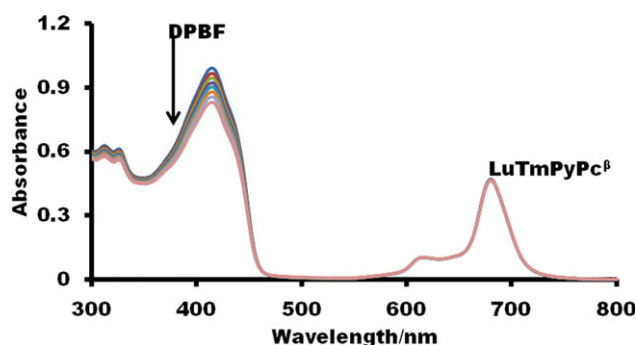


**Figure 3.** UV–visible absorption spectra changes for the conversion of DPBF by excited state singlet oxygen using complex **8** in DMF. [Color figure can be viewed in the online issue, which is available at [wileyonlinelibrary.com](http://wileyonlinelibrary.com).]

using chemical methods. In DMF, DPBF was used as singlet oxygen quencher and unsubstituted zinc phthalocyanine was used as standard. Figure 3, shows the degradation profile of DPBF in the presence of complex **8** upon Q band irradiation. Phthalocyanine did not degrade indicating that it is quite stable to the visible light irradiation under the conditions used for singlet oxygen studies. The singlet oxygen quantum yield was determined to be 0.64 in DMF, Table I. For the phthalocyanine within the PS polymer matrix, ADMA was used as singlet oxygen quencher and a quantum yield of 0.15 (Table I) was obtained. Such lowering of the singlet oxygen yield has been explained in the context that the phthalocyanine is constrained within a solid matrix.<sup>33</sup> The decrease in the singlet oxygen quantum yield could also be explained in the context that water absorbs where singlet oxygen energy levels are located,<sup>34</sup> hence water has a high quenching effect on singlet oxygen, decreasing the values of its quantum yield. Also the singlet oxygen quantum yields determined for the fibers are an estimate as discussed above.

### Fluorescence Behavior of the Phthalocyanine with Solid Polymer Fibers

The fluorescence behaviors of the phthalocyanines within the fibers were assessed by taking fluorescence micrographs on exciting the functionalized fibers in the Q band region with a high-voltage mercury lamp, Figure 4. The fluorescence of unsubstituted zinc phthalocyanine, a known fluorophore<sup>24</sup> when functionalized on the various polymers, was used as reference for the other phthalocyanine functionalized fibers. Fluorescence is judged by the red color of the fiber under illumination. Polymer fibers functionalized with unsubstituted zinc phthalocyanine fluoresce [Figure 4(a–d)] even though those of polyurethane fibers seem to be fused together, under excitation. This is consistent with the fluorescence behavior of the phthalocyanine in solution and suggests that the molecules are quite

**Table I.** Fluorescence and Singlet Oxygen Quantum Yields of MPc Derivatives

Complex	$\Phi_F$ (in DMF)	$\Phi_\Delta$		Polymer used
		Solution <sup>a</sup> DMF	Fiber (in water) <sup>a</sup>	
ZnPc	0.30 [23]	0.56 [24,25]	0.25 [TW]; 0.13 [16]	PSU; PS
1	0.23 [18]	0.56 [18]	0.24 [TW]	PSU
2	0.22 [18]	0.59 [18]	0.21 [TW]	PSU
3 [15]	<0.01	0.17	<sup>c</sup>	PAA
4 [15]	<sup>b</sup>	0.29	<sup>c</sup>	PAA
5 [21]	0.01	0.33	0.11	PUR
6 [17]	<0.01	0.68	0.28	PS
7 [17]	0.017	0.62	0.17; 0.26	PS; PSU
8 [TW]	0.01	0.64	0.15	PS
9 [16]	<0.01	0.71	0.22	PS

References in square brackets.

<sup>a</sup>TW = this work, <sup>b</sup>Too low to be detected, <sup>c</sup>No value determined—polymer dissolves in water.

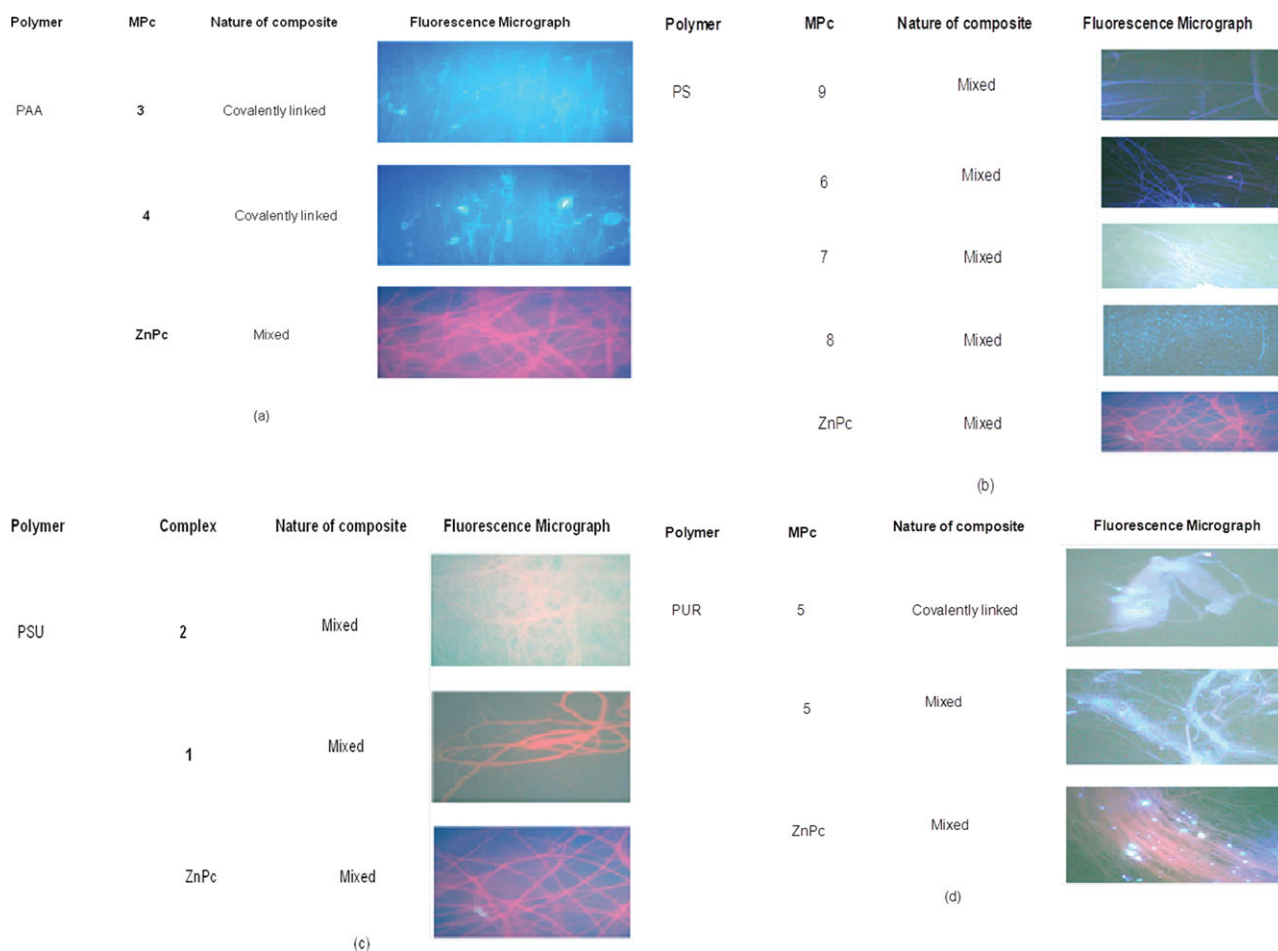


**Figure 4.** Composition and nature of the functionalized fibers and their corresponding fluorescence micrographs with (a) PAA, (b) PS, (c) PSU, and (d) PUR polymers. [Color figure can be viewed in the online issue, which is available at [wileyonlinelibrary.com](http://wileyonlinelibrary.com).]

dispersed within the polymer matrices and not stacked together as in the solid state that are usually not emissive.<sup>35</sup> For complex **3** functionalized fibers, no or very low fluorescence has been reported due to the quenching effects of the amino group,<sup>36</sup> hence no fluorescence is observed in Figure 4(a). The same will apply to complex **4** which will also be affected by the heavy atom effect, Figure 4(a). For the other ZnPc derivatives (complexes **1** and **2**) fluorescence has been reported in DMF solution.<sup>18</sup> Their fluorescence has been maintained (though not as strong as that for unsubstituted ZnPc) in the functionalized fibers as shown in their fluorescence micrographs, Figure 4(c). In general, LuPc complexes **4–9** have lower fluorescence quantum yield values than ZnPc derivatives due to the heavy atom effect of the central Lu atom.

The Lu phthalocyanine complexes are generally not emissive in solution due to the large size of the diamagnetic lutetium atom which encourages intersystem crossing to the triplet state.<sup>15,21,22</sup> Thus as shown in Figure 4(b, d), the fluorescence micrographs of the corresponding functionalized polymer fibers containing the various Lu phthalocyanine complexes do not show the characteristic fluorescence exhibited by those containing the unsubstituted zinc phthalocyanine, Figure 4(a–d). Thus whether the phthalocyanine is embedded within the polymer matrix through

electrostatic or ionic attraction as well as being covalently linked its solution fluorescence characteristics is maintained.

#### Suitability of the Polymer Fibers in Photocatalytic Application in Aqueous Solutions

The solvent compatibility of the functionalized fibers is paramount in their application in a particular medium. Thus we assessed the possibility of using the various functionalized fibers for photoconversion of environmental organic pollutants (4-CP, 4-NP and methyl orange) in aqueous media.

Polymer fibers from polyacrylic acid were found not to be suitable for application involving aquatic systems. This is because the polymer dissolved extensively in water to give a gelatinous solution.

For PUR/complex **5** covalently functionalized fiber, photoactivity has been reported to be maintained.<sup>21</sup> The functionalized fibers could not degrade any of the pollutants to any detectable extent, even after 12 h of irradiation. Equally, when the phthalocyanine and the polymer were merely mixed, not covalently linked and electrospun into fibers, no degradation of the pollutants occurred. Further, we functionalized the polyurethane polymer fibers with the very photoactive complexes **9**<sup>22</sup> and **(6)**<sup>17</sup> and applied in the catalysis. Once again no significant

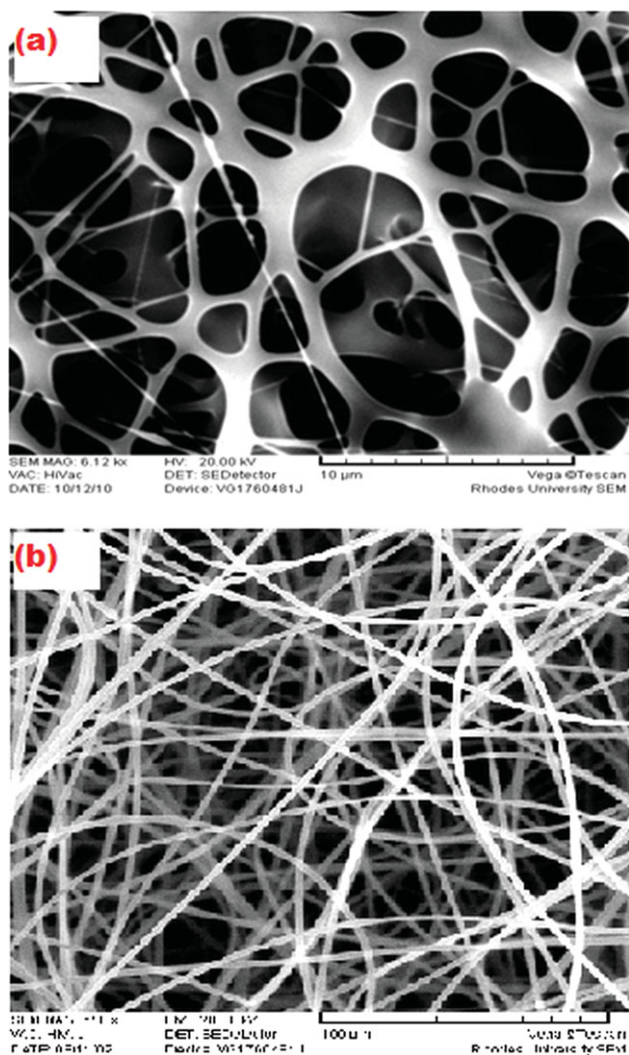


**Figure 5.** Fiber mats for (a) polyurethane polymer (b) polystyrene polymer.

degradation of any of the pollutants was observed. This we believe is primarily due to the morphology and nature of the fiber mat which shows that the fibers are fused together as compared to those of polystyrene, Figure 5. Thus they are not porous enough for sufficient interaction of reacting species with the embedded photoactive phthalocyanine molecules within the fiber matrix.

On the other hand, functionalized polymer fibers of polystyrene (PS) and polysulfone (PSU) were found to be insoluble in water and cotton-like, being quite porous, thus more promising in the photocatalytic application in aqueous systems.

ZnPc and a LuPc complex **7** were studied in both PSU and PS. Table I shows that higher singlet oxygen quantum yields are generated for ZnPc in PSU than in PS. PS has a more extensive aromatic system than PSU. The ZnPc could be more tightly constrained within PS than PSU, resulting in better photochemical and photophysical behavior within the PSU fiber matrix. The same behavior was observed for a LuPc complex **7**, where higher singlet oxygen quantum yield ( $\Phi_{\Delta}$ ) was obtained within

the PSU fiber matrix ( $\Phi_{\Delta} = 0.26$ ) compared to that in PS in fiber matrix ( $\Phi_{\Delta} = 0.17$ ). High singlet oxygen quantum yields were observed for complex **6** within the PS fiber compared to all the other complexes. This behavior was also observed in solution; Table I. The difference between complexes **6** and **9** is in the position of the substituent (peripheral versus nonperipheral, respectively).

### Application of Polystyrene (PS)-Phthalocyanine Functionalized Fibers for Photoconversion of Environmental Pollutants in Aqueous Medium

Phenolic compounds and azo dyestuff are ubiquitous pollutants which are introduced into the natural water resources from the effluents of a variety of chemical industries such as phenol manufacturing, pharmaceuticals, paint, dyeing, textile, wood, petrochemical and pulp mills.<sup>37–39</sup> As a result, aquatic organisms including fish are subjected to these pollutants.<sup>40</sup>

The reactivity of phenolic compounds can be drastically affected by the electronic nature of substituents and by their positions in the aromatic ring.<sup>41,42</sup> Thus the extent to which each of these phenolic pollutants can be removed from the environment by a particular catalytic system is greatly influenced by their reactivity. In this work we assessed the ease of photodegradation of the two substituted phenolic compounds (4-CP and 4-NP) using the polystyrene functionalized fibers (PS/(**6**), PS/(**7**), PS/(**8**), PS/(**9**)), these are photoactive with  $\Phi_{\Delta} = 0.28, 0.17, 0.15,$  and  $0.22,$  respectively, Table I. In general, it was observed that photodegradation of 4-chlorophenol occurs faster than for 4-nitrophenol, with higher  $k_{\text{obs}}$  (and lower half-lives) values for similar initial concentrations, Table II. This is consistent with reported studies using other sensitizers.<sup>41</sup> The reported studies showed that the kinetics of the photocatalytic degradation of phenolic pollutants is faster for those containing electron-donating substituents. The  $-\text{Cl}$  group in our case is more electron donating than the  $-\text{NO}_2$  group which accounts for our observed trend.

Furthermore, as illustrated in Figure 6, a solution of  $2.72 \times 10^{-4} \text{ M}$  4-chlorophenol could be degraded completely within two and half hours of irradiation with PS/complex (**6**) fibers, while sample solution of 4-nitrophenol of the same concentration and under similar experimental condition was not completely degraded.

The use of these functionalized fibers for the photoconversion of methyl orange, an azo dye, showed much more slow reaction kinetics than those of the phenolic compounds. Such slow photoconversion has been reported before.<sup>43,44</sup> In all cases it was observed that the initial reaction rates increases with the initial concentration of the analyte. This is consistent with basic reaction kinetics laws.

Comparing complexes **7** and **8** containing the same substituent (and embedded in PS fiber, and the latter the quaternized version of the former) shows in general larger  $k_{\text{obs}}$  values are observed for the unquaternized derivatives with correspondingly smaller half-lives. No leaching of the water soluble quaternized derivative from the fiber was observed, hence the differences may be due to slightly larger singlet oxygen quantum yield of

**Table II.** Kinetic Data for PS Fibers with Various Initial Concentrations of the Pollutants

Functionalized fiber	Pollutant	Initial conc. $\times 10^{-4}M$	$k_{obs} \times 10^{-2}$ $min^{-1}$	Initial rate $\times 10^{-6}$ $molL^{-1} min^{-1}$	Half-life (min)
PS/complex <b>6</b>	4-CP	1.2	3.00	3.60	23.10
	4-NP		1.38	1.66	50.20
	MO		0.61	0.73	113.63
	4-CP	2.0	2.11	4.22	32.85
	4-NP		1.22	2.44	56.80
	MO		0.46	0.91	150.68
	4-CP	2.5	1.90	4.76	36.48
	4-NP		1.11	2.78	61.90
	MO		0.40	1.00	173.29
PS/complex <b>7</b>	4-CP	1.2	1.93	2.31	35.91
	4-NP		1.07	1.26	64.78
	MO		0.38	0.45	182.41
	4-CP	2.0	1.80	3.60	38.51
	4-NP		1.05	2.14	66.01
	MO		0.36	0.72	192.54
	4-CP	2.5	1.58	3.95	43.87
	4-NP		0.95	2.38	72.96
	MO		0.34	0.85	203.87
PS/complex <b>8</b>	4-CP	1.2	1.83	2.20	37.88
	4-NP		0.98	1.17	70.73
	MO		0.38	0.45	182.41
	4-CP	2.0	1.77	3.55	39.16
	4-NP		0.97	1.94	71.46
	MO		0.34	0.68	203.87
	4-CP	2.5	1.58	3.95	43.87
	4-NP		0.92	2.31	75.34
	MO		0.32	0.80	216.61
PS/complex <b>9</b>	4-CP	1.2	2.62	3.14	26.46
	4-NP		1.09	1.31	63.59
	MO		0.53	0.64	130.78
	4-CP	2.0	1.98	3.95	35.00
	4-NP		1.03	2.06	67.30
	MO		0.38	0.76	182.41
	4-CP	2.5	1.71	4.27	40.54
	4-NP		1.01	2.53	68.63
	MO		0.36	0.91	192.54
PS/ZnPc [16] <sup>a</sup>	4-CP	2.7	0.05	0.14	1386.30

<sup>a</sup>Reference in brackets.

the unquaternized complex **7**. Comparing complexes **6** and **9** (embedded in PS fiber) containing the same substituent, but peripherally and nonperipherally substituted, respectively, shows larger  $k_{obs}$  values for **6** with correspondingly smaller half-lives. The values correspond to the singlet oxygen quantum yields as summarized in Table III. Thus factors which affect the production of singlet oxygen by the Pc within the fiber, will affect the effectiveness of the functionalized fibers for the phototransformation of pollutants.

ZnPc embedded in PS fiber shows much slower kinetics than LuPc derivatives, due to the smaller size of Zn, Table II.

The possibility of the phthalocyanines embedded in the electrospun fiber leaching out into the aqueous sample solutions was investigated. As observed in Figure 6(C), there were no detectable absorptions in the Q band region (650–750 nm) corresponding to the embedded phthalocyanine during the photocatalytic processes. This suggests that the phthalocyanines are

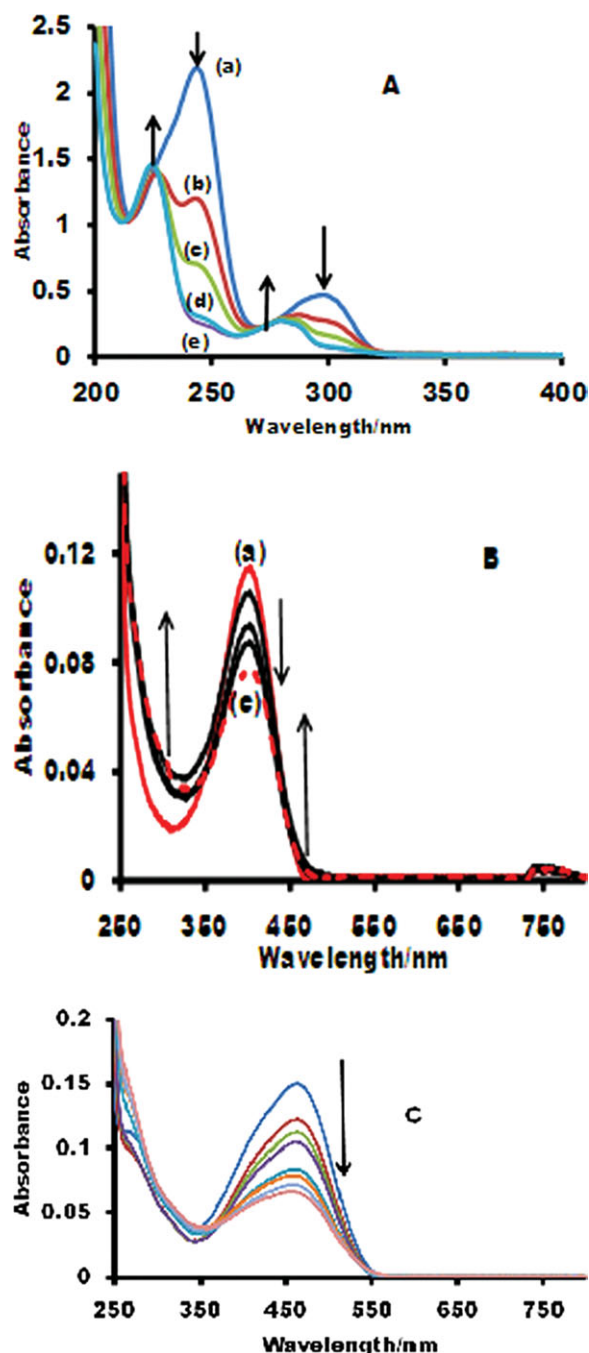


**Figure 6.** Electronic absorption spectral changes of (A) 4-CP ( $2.72 \times 10^{-4} \text{ mol L}^{-1}$ ), (B) 4-NP ( $2.72 \times 10^{-4} \text{ mol L}^{-1}$ ) and (C) methyl orange ( $1.5 \times 10^{-4} \text{ mol L}^{-1}$ ) during visible light photocatalysis in the presence of PS/complex 6 for (A) and (B) and PSU/complex 2 for (C) fiber; at times: (a) 0, (b) 1, (c) 1.5, (d) 2, (e) 2.5 h. [Color figure can be viewed in the online issue, which is available at [wileyonlinelibrary.com](http://www.wileyonlinelibrary.com).]

tightly bound within the polymer matrices. Even the water soluble Pcs 2 and 8 did not leach out from the fiber. The photodegradation of the analytes therefore involves their diffusion to the fiber to be oxidized by singlet oxygen generated by the embedded Pc. This is followed by the diffusion of the products back into solution, hence the observed absorption spectra of the

products of the oxidation. We have previously<sup>16,17</sup> employed Langmuir–Hinshelwood (L–H) kinetic model, which has been successfully used to describe solid–liquid reactions. This model was employed for the analysis of interaction of fibers functionalized with various phthalocyanines with 4-chlorophenol and 4-nitrophenol. Linear plots were obtained showing that the catalysis occurs appreciably on the surface of the functionalized fiber.

#### Application of Polysulfone (PSU)-Phthalocyanine Functionalized Fibers for Photocatalysis in Aqueous Medium

Zinc phthalocyanines complexes (ZnPc, complexes 1 and 2) and LuPc derivative 7, were used as examples to functionalize polysulfone polymer fibers for the photoconversion of 4-CP, 4-NP, and methyl orange. The fibers were generally insoluble in water and quite porous cotton-like in morphology and thus promising materials for photocatalytic application in aquatic systems.

Complexes 1 and 2 have been reported to be photoactive with the quantum yield of singlet oxygen production 0.56 and 0.59, respectively in DMF,<sup>18</sup> Table I, which are quite reasonable values for zinc phthalocyanines in DMF.<sup>26,45</sup> Complex 7 has singlet oxygen quantum yield of 0.62 in DMF.<sup>17</sup>

The singlet oxygen quantum yields in water were estimated to be  $\Phi_{\Delta} = 0.21$  for PSU/complex 2 fiber, 0.24 for PSU/complex 1, 0.25 for PSU/ZnPc and 0.26 PSU/complex 7 fibers. The lower singlet oxygen quantum yield for complexes 1, 2, 7 and ZnPc within the solid fiber matrices (and in water) compared to those in DMF (at  $\Phi_{\Delta} = 0.56, 0.59, 0.62,$  and  $0.56,$  respectively) could be due the reasons given above for complex 8. The efficiency of the photoconversion of 4-CP, 4-NP, and methyl orange using PSU/ZnPc, PSU/complex 1, PSU/complex 2 fibers, Table IV, follow similar trends as those of polystyrene functionalized fibers. Again 4-chlorophenol proved to be much more susceptible to photodegradation than 4-nitrophenol with methyl orange been quite difficult to photodegrade as judged by higher  $k_{\text{obs}}$  values and shorter half-lives for 4-CP, Table IV. The PSU/ZnPc and PSU/complex 1 fibers showed a much more promising photosensitizing material than PSU/complex 2 fibers possibly due to the difference in singlet oxygen quantum yields, Table III. Again this shows that unquaternized derivatives show better activity than quaternized counter-parts as observed above for the LuPc derivatives. Table IV shows that even when PSU (rather than PS) is employed as a polymer, LuPc still shows better kinetics for the degradation of pollutants compared to ZnPc, for the

**Table III.** Kinetic Data for Phototransformation of 4-CP at Initial Concentration of  $2 \times 10^{-4} \text{ mol L}^{-1}$  using Different Functional Fibers

Functionalized fiber	$k_{\text{obs}} \times 10^{-2} \text{ min}^{-1}$	$\Phi_{\Delta}$ in fiber
PS/ZnPc	0.6	0.13
PS/6	2.11	0.28
PS/7	1.80	0.17
PS/8	1.77	0.15
PS/9	1.98	0.22
PSU/1	2.01	0.24
PSU/2	1.75	0.21
PSU/ZnPc	1.75	0.25

**Table IV.** Kinetic Data for PSU Fibers with Various Initial Concentrations of the Pollutants

Functionalized fiber	Pollutant	Initial conc. $\times 10^{-4}$ molL $^{-1}$	$k_{\text{obs}} \times 10^{-2}$ min $^{-1}$	Initial rate $\times 10^{-6}$ molL $^{-1}$ min $^{-1}$	Half-life (min)
PSU/complex 1	4-CP	1.2	2.83	3.39	24.49
	4-NP		1.21	1.45	57.28
	MO		0.62	0.74	111.80
	4-CP	2.0	2.01	4.02	34.48
	4-NP		1.19	2.37	58.24
	MO		0.45	0.89	154.03
	4-CP	2.5	1.68	4.21	41.26
	4-NP		1.05	2.63	66.01
	MO		0.38	0.94	182.41
PSU/complex 2	4-CP	1.2	2.24	2.69	30.94
	4-NP		1.09	1.31	63.59
	MO		0.50	0.60	138.63
	4-CP	2.0	1.75	3.50	39.61
	4-NP		0.99	1.98	70.01
	MO		0.41	0.82	169.06
	4-CP	2.5	1.64	4.10	42.27
	4-NP		0.81	2.02	85.57
	MO		0.37	0.93	187.34
PSU/ZnPc	4-CP	1.2	2.34	2.81	29.62
	4-NP		1.13	1.36	61.34
	MO		0.50	0.60	138.63
	4-CP	2.0	1.75	3.50	39.61
	4-NP		1.02	2.03	67.96
	MO		0.42	0.83	165.04
	4-CP	2.5	1.64	4.11	42.27
	4-NP		0.85	2.13	81.55
	MO		0.37	0.93	187.34
PSU/complex 7	4-CP	1.2	2.84	3.41	24.41
		2.0	2.07	4.14	33.49
		2.5	1.81	4.53	38.30

reasons provided above. This is clearly seen by comparing the kinetic data for the degradation of 4-CP using PSU/complex 7 and those functionalized with ZnPc and its derivatives, Table IV.

### Products of Photocatalytic Reactions

The catalytic products of 4-chlorophenol and 4-nitrophenol were identified with gas chromatography using standards. Also sample solutions were injected directly into ion trap mass spectrometer to further ascertain the identity of the products.

In the case of 4-chlorophenol, three degradation products were obtained, Figure 7: benzoquinone, hydroquinone and 4,4'-oxydiphenol. The benzoquinone photo-product has been reported<sup>8</sup> to originate from the reaction of singlet oxygen with 4-chlorophenol (Type II mechanism) while hydroquinone and any dimeric product originate from electron transfer reactions (Type I mechanism). Thus photoactivity of the functionalized fibers involves both singlet oxygen and radicals.

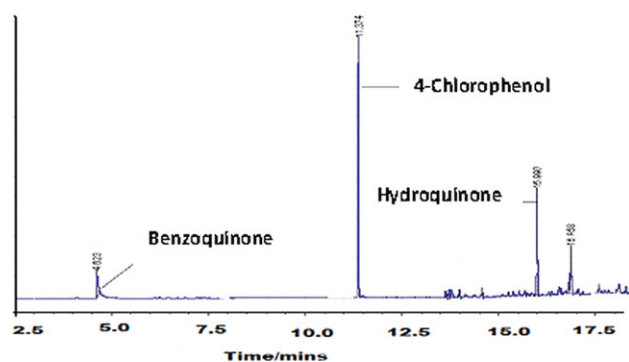


**Figure 7.** Gas chromatographic traces of 4-chlorophenol after being photolyzed 12 h in the presence of PS/complex 9 functionalized fiber. [Color figure can be viewed in the online issue, which is available at [wileyonlinelibrary.com](http://wileyonlinelibrary.com).]

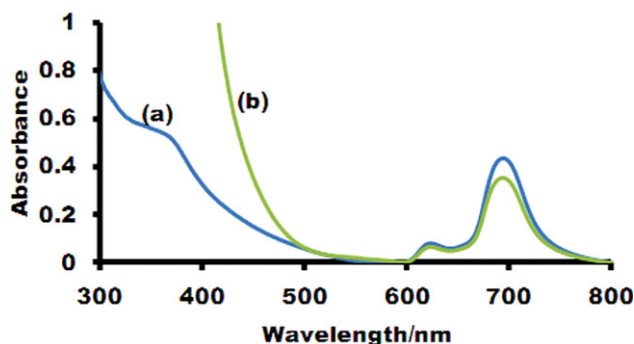


**Figure 8.** UV-vis spectra of 10 mg of PS/complex 6 functionalized fiber (a) not used in catalysis (b) used in catalysis (time 12 h), each dissolved in 4 mL of THF. [Color figure can be viewed in the online issue, which is available at [wileyonlinelibrary.com](http://wileyonlinelibrary.com).]

In the case of 4-nitrophenol, benzoquinone, hydroquinone, and 4-nitrocatechol were the products obtained also suggesting the involvement of both Type I and II photodegradation mechanisms of the sensitizers.

Mass spectral analysis of the photodegradation products of methyl orange showed the presence in the solution of a coupling product at  $m/z = 293$  amu as well as a series of oligopolymeric products ( $m/z = 324, 325, 397, 398$  amu). Similar degradation products have been reported for oxidative degradation of methyl orange, and the coupling product was identified as 2-amino-5-(3-hydroxy-4-oxo-cyclohexa-2,5-dienylideneamino)-benzene sulfonic acid ( $m/z = 293$  amu) and the oligopolymeric product ( $m/z 325$ ) was identified as poly(catechol).<sup>46</sup>

#### Reusability of the Functionalized Fibers

The photostability of imbedded sensitizer is an important factor for the application of such fabric materials for photocatalysis. Therefore the photostability of phthalocyanines within the fiber matrices were assessed by observing the Q-band absorption of an equivalent amount (10 mg) of the fibers before and after catalysis, both dissolved in equal volume of THF (4 mL), Figure 8, using PS/complex 6 fiber as an example. As indicated, the decrease in the absorption band after the photolysis suggests that the phthalocyanine photodegrades slightly upon continuous irradiation for 12 h. This could account for the decrease in the reaction rates when the functionalized fibers were used for repetitive conversion of the 4-nitrophenol. Nonetheless, the fiber could be reused for at least three cycles for degradation of 4-nitrophenol. FT-IR analysis of the fibers before and after irradiation showed no apparent structural changes in the components. Also scanning electron microscopic (SEM) images of the fibers after use, indicate that the average diameters remained virtually the same. However the strands of fibers became more closely compressed than before. Thus there was reduced porosity in the fiber mats and could also account for the reduced degradation rate of the analytes during reuse of the fibers.

In the case of the polysulfone functionalized fiber, the phthalocyanine complexes were quite stable under the applied irradiation light intensity. However, the functionalized fibers folded up into a hard lump when they were dried after the first cycle of catalysis and could not be applied again.

## CONCLUSIONS

In this work various polymers incorporating a series of zinc and lutetium phthalocyanine complexes were electrospun into fibers and used for the photoconversion of azo dye and phenolic compounds in aqueous media. Polystyrene and polysulfone functionalized fibers were found to be promising fabric materials for the photodegradation of 4-chlorophenol, 4-nitrophenol, and the methyl orange with the ease of conversion generally in the order 4-chlorophenol > 4-nitrophenol > methyl orange. Polystyrene fibers were found to be reusable for at least three times.

## ACKNOWLEDGMENTS

This work was supported by the Department of Science and Technology (DST) and National Research Foundation (NRF) of South Africa through DST/NRF South African Research Chairs Initiative for Professor of Medicinal Chemistry and Nanotechnology and Rhodes University.

## REFERENCES

- Sugawara, M.; Kojima, K.; Sazawa, H.; Umezawa, Y. *Anal. Chem.* **1987**, *50*, 2842.
- Shishiyanu, S. T.; Shishiyanu, T. S.; Lupan, O. I. *Sens. Actuators B* **2005**, *107*, 379.
- Pichon, V.; Chapuis-Hugon, F. *Anal. Chim. Acta* **2008**, *622*, 48.
- Legrini, O.; Oliveiris, E. A.; Braun, M. *Chem. Rev.* **1993**, *93*, 671.
- Honigsmann, H.; Jori, G.; Young, A. R. *The Fundamental Bases of Phototherapy*; OEMF: Milan, **1996**.
- Ali, H.; van Lier, J. E. *Chem. Rev.* **1999**, *99*, 2379.
- Suri, R. P. S.; Liu, J.; Hand, D. W.; Crittenden, J. C.; Perram, D. L.; Mullins, M. E. *Water Environ. Res.* **1993**, *65*, 665.
- Silva, E.; Pereira, M. M.; Burrows, H. D.; Azenha, M. E.; Sarakha, M.; Bolte, M. *Photochem. Photobiol. Sci.* **2004**, *3*, 200.
- Morgado, J.; Friend, R. H.; Cacialli, F.; Chuah, B. S.; Moratti, S. C.; Holmes, A. B. *J. Appl. Phys.* **1999**, *86*, 6392.
- Yang, Y.; Pei, Q. *J. Appl. Phys.* **1997**, *81*, 3294.
- Ge, J. J.; Hou, H.; Li, Q.; Grahams, M. J.; Greiner, A.; Reneker, D. H.; Harris, F. W.; Cheng, S. Z. D. *J. Am. Chem. Soc.* **2004**, *126*, 15754.
- Zussman, E.; Yarin, A. L.; Bazilevsky, A. V.; Avrahami, R.; Feldman, M. *Adv. Mater.* **2006**, *18*, 348.
- Mosinger, J.; Lang, K.; Kubàt, P.; Sýkora, J.; Hof, M.; Plíštil, L.; Mosinger, B., Jr. *J. Fluoresc.* **2009**, *19*, 705.
- Tang, S.; Shao, C.; Liu, Y.; Li, S.; Mu, R. *J. Phys. Chem. Solids* **2007**, *68*, 2337.
- Zugle, R.; Nyokong, T. *J. Macromol. Sci. Pure Appl. Chem.* **2012**, *49*, 279.
- Zugle, R.; Antunes, E.; Khene, S.; Nyokong, T. *Polyhedron* **2012**, *33*, 74.
- Zugle, R.; Nyokong, T. *J. Mol. Cat. A Chem.* **2012**, *358*, 49.

18. Scalise, I.; Durantini, E. N. *Bioorg. Med. Chem.* **2005**, *13*, 3037.
19. Spesia, M. B.; Caminos, D. A.; Pons, P.; Durantini, E. N. *Photodiag. Photodyn. Therapy* **2009**, *6*, 52.
20. Achar, B. N.; Fohlen, G. M.; Parker, J. A.; Keshavayya, J. *Polyhedron* **1987**, *6*, 1463.
21. Zuggle, R.; Litwinski, C.; Torto, N.; Nyokong, T. *N. J. Chem.* **2011**, *35*, 1588.
22. Zuggle, R.; Litwinski, C.; Nyokong, T. *Polyhedron* **2011**, *30*, 1612.
23. Fery-Forgues, S.; Lavabre, D. *J. Chem. Ed.* **1999**, *76*, 1260.
24. Shen, T.; Yuan, Z.; Xu, H. *Dyes Pigment* **1989**, *11*, 77.
25. Zhang, X.-E.; Xu, H.-J. *J. Chem. Soc. Faraday Trans.* **1993**, *89*, 3347.
26. Nyokong, T. *Coord. Chem. Rev.* **2007**, *251*, 1707.
27. Ogunsipe, A.; Maree, D.; Nyokong, T. *J. Mol. Struct.* **2003**, *650*, 131.
28. Ogunsipe, A.; Nyokong, T. *J. Photochem. Photobiol. A* **2005**, *173*, 211.
29. Foote, C. S. In *Singlet Oxygen*; Wasserman, H. H., Murray, R. W., Eds.; Academic Press: New York, **1979**; p 139.
30. Smith, T. D.; Livoriness, J.; Taylor, H.; Pilbrow, J. R.; Sinclair, G. R. *J. Chem. Soc. Dalton. Trans.* **1983**, 1391.
31. Yuan, X. Y.; Zhang, Y. Y.; Dong, C.; Sheng, J. *Polym. Int.* **2004**, *53*, 1704.
32. Tomachynski, L. A.; Tretyakova, I. N.; Chernii, V. Y.; Volkov, S. V.; Kowalka, M.; Legendziewicz, J.; Greasymchuk, Y. S.; Radzki, S. *Inorg. Chim. Acta* **2008**, *361*, 2569.
33. Lang, K.; Mosinger, J.; Wagnerová, D. M. *Coord. Chem. Rev.* **2004**, *248*, 321.
34. Ogunsipe, A.; Chen, J.-Y.; Nyokong, T. *N. J. Chem.* **2004**, *28*, 822.
35. Ngai, T.; Zhang, G.; Li, X.; Ng, D. K. P.; Wu, C. *Langmuir* **2001**, *17*, 1381.
36. Zhang, X.-F.; Li, X.; Niu, L.; Sun, L.; Liu, L. *J. Fluoresc.* **2009**, *19*, 947.
37. Fleeger, J. W.; Carman, K. R.; Nisbet, R. M. *Sci. Total Environ.* **2003**, *317*, 207.
38. Mukherjee, D.; Bhattacharya, S.; Kumar, V.; Moitra, J. *Biomed. Environ. Sci.* **1990**, *3*, 337.
39. Mukherjee, D.; Guha, D.; Kumar, V.; Chakrabarty, S. *Aquat. Toxicol.* **1991**, *21*, 29.
40. Shalaby, A. M.; Mousa, M. A.; Tag Elden, H. A. *Egypt J. Aquatic Biol. Fisheries* **2007**, *11*, 145.
41. Parra, S.; Olivero, J.; Pacheco, L.; Pulgarin, C. *Appl. Catal. B Environ.* **2003**, *43*, 293.
42. D'Oliveira, J. C.; Minero, C.; Pelizzetti, E.; Pichat, P. *J. Photochem. Photodiol. Chem. A* **1993**, *72*, 261.
43. Abdullah, M.; Low, G. K. C.; Mathews, R. W. *J. Phys. Chem.* **1990**, *94*, 6820.
44. Hou, M.; Li, F.; Liu, X.; Wang, X.; Wan, H. *J. Hazard Mater.* **2007**, *145*, 305.
45. Redmond, R. W.; Gamlin, J. N. *Photochem. Photobiol.* **1999**, *70*, 391.
46. Zille, A.; Górnacka, B.; Rehorek, A.; Cavaco-Paula, A. *Appl. Environ. Microbiol.* **2005**, *71*, 6711.